and increasing the conductance. An example of the formation of channel–Fab′ crosslinked species and their liberation upon the addition of digoxin is shown in Fig. 4. A control is also shown in which the addition of thyroxine fails to elicit a response. The absence of biotins on the lipid tether, the absence of the streptavidin linker or the correctly targeted Fab′ eliminates the response. A quantitative measure of analyte concentration may be obtained from either the absolute initial rate of admittance increase, or the equilibrium fractional admittance change (see Supplementary Information). These are essentially proportional to each other over the sensitivity range of the competitive assay. The range may be adjusted by varying the immobilised Fab′ surface density.

By varying the nature and type of receptor in the ICS biosensor, we have applied the technique to blood typing, the detection of bacteria, virus particles, DNA, drugs, antibodies and electrolytes. Receptors include antibodies, enzymes, DNA, binding proteins and synthetic ligands. The ion-transport properties of channels and ionophores other than gramicidin have also been studied[17,18]. For example, we have incorporated the K^+ ionophore valinomycin into a tethered membrane and successfully measured potassium concentration over physiologically relevant concentrations. The biosensor functions in human serum, plasma and whole blood. The biosensor may be assembled and measured on electrodes of dimensions from square centimetres to square micrometres. As the membrane area is decreased, the membrane leakage conductance decreases proportionally, but the conductance per channel remains constant. This means that with small electrodes (<30 μm diameter) it becomes possible to resolve the current transients associated with individual channels. Operation of the biosensor under these conditions of low channel density, coupled with the use of multi-electrode arrays of such membranes, promises to increase significantly the sensitivity of the device. □

Received 14 November 1996; accepted 14 April 1997

1. Scheller, F. W., Schubert, F. & Fedrowitz, J. (eds) *Frontiers in Biosensorics* Vols I & II (Birkhauser, Berlin, 1996).
2. Avrone, E. & Rospars, J. P. Modelling insect olfactory neurone signaling by a network utilising disinhibition. *Biosystems* **36,** 101–108 (1995).
3. Reiken, S. R. *et al*. Bispecific antibody modification of nicotine acetycholine receptors for biosensing. *Biosens. Bioelectron.* **11,** 91–102 (1996).
4. Koeppe, R. E. & Andersen, O. S. Engineering the gramicidin channel. *Annu. Rev. Biophys. Biomol. Struct.* **25,** 231–258 (1996).
5. McConnell, H. M., Watts, T. H., Weis, R. M. & Brian, A. A. Supported planar membranes in studies of cell-cell recognition in the immune system. *Biochim. Biophys. Acta* **864,** 95–106 (1986).
6. Florin, E.-L. & Gaub, H. E. Painted supported lipid membranes. *Biophys. J.* **64,** 375–383 (1993).
7. Lang, H., Duschl, C. & Vogel, H. A new class of thiolipids for the attachment of lipid bilayers on gold surfaces. *Langmuir* **10,** 197–210 (1994).
8. Steizle, M., Weismuller, G. & Sackmann, E. On the application of supported bilayers as receptive layers for biosensors with electrical detection. *J. Phys. Chem.* **97,** 2974–2981 (1993).
9. Plant, A. L., Gueguetchkeri, M. & Yap, W. Supported phospholipid/alkanethiol biomimetic membranes: insulating properties. *Biophys. J.* **67,** 1126–1133 (1994).
10. Folkers, J. P., Laibinis, P. E., Whitesides, G. M. & Deutch, J. Phase behaviour of two-component self-assembled monolayers of alkanethiolates on gold. *J. Phys. Chem.* **98,** 563–571 (1994).
11. Steinem, C., Janschoff, A., Ulrich, W. P., Sieber, M. & Galla, H. J. Impedance analysis of supported lipid bilayer membranes: a scrutiny of different preparation techniques. *Biochem. Biophys. Acta* **1279,** 169–180 (1996).
12. Lu, X. D., Ottova, A. L. & Tien, H. T. Biophysical aspects of agar-gel supported bilayer lipid membranes: a new method for forming and studying planar bilayer lipid membranes. *Bioelectrochem. Bioenerget.* **39,** 285–289 (1996).
13. Heysel, S., Vogel, H., Sanger, M. & Sigrist, H. Covalent attachment of functionalised lipid bilayers to planar waveguides for measuring protein binding to biomimetic membranes. *Protein Sci.* **4,** 2532–2544 (1995).
14. Rickert, J., Weiss, T., Kraas, W., Jung, G. & Gopel, W. A new affinity biosensor: self-assembled thiols as selective monolayer coatings of quartz crystal microbalances. *Biosens. Bioelectron.* **11,** 591–598 (1996).
15. Sackmann, E. Supported membranes: scientific and practical applications. *Science* **271,** 43–48 (1996).
16. Stetter, K. O. Hypothermophilic procaryotes. *FEMS Microbiol. Rev.* **18,** 149–158 (1996).
17. Hladky, S. B., Leung, J. C. H. & Fitzgerald, W. The mechanism of ion conduction by valinomycin-analysis of charge pulse responses. *Biophys. J.* **69,** 1758–1772 (1995).
18. Nikolelis, D., Siontorou, C. G., Krull, U. J. & Katrivanos, P. L. Ammonium ion minisensors from self-assembled bilayer lipid membranes using gramicidin as an ionophore. Modulation of ammonium selectivity by Platelet Activating Factor. *Anal. Chem.* **68,** 1735–1741 (1996).

Supplementary Information is available on *Nature*'s World-Wide Web site (http://www.nature.com) or as paper copy from Mary Sheehan at the London editorial office of *Nature*.

Acknowledgements. This work was supported by the Australian Industrial Research & Development Board and the Cooperative Research Centres (CRC) program. The partner organisations within the CRC for Molecular Engineering & Technology are the Commonwealth Scientific & Industrial Research Organisation, the University of Sydney and the Australian Membrane & Biotechnology Research Institute.

Correspondence and requests for materials should be addressed to B.A.C. (e-mail: bcornell@ambri.com.au).

Synthesis and X-ray structure of dumb-bell-shaped C_{120}

Guan-Wu Wang*, Koichi Komatsu*, Yasujiro Murata* & Motoo Shiro†

* *Institute for Chemical Research, Kyoto University, Uji, Kyoto 611, Japan*
† *Rigaku Corporation, 3-9-12 Matsubara-cho, Akishima, Tokyo 196, Japan*

The discovery and large-scale synthesis of fullerenes have aroused interdisciplinary interest in these closed-cage molecules[1–6]. C_{60} can be photopolymerized into a form in which the cages are thought to be linked by cyclic C_4 units in a [2 + 2] cycloaddition[7], provoking theoretical studies of the C_{60} dimer[8–15], the smallest subunit of such a polymer. The C_{60} dimers $C_{120}O$ (refs 16, 17), $C_{121}H_2$ (ref. 17) and $C_{120}O_2$ (ref. 18) have been reported, in which the two C_{60} molecules are linked by, respectively, a furan group, a cyclopentane ring and a cyclobutane ring plus two oxygen bridges; but the simplest dimer, C_{120} linked by a cyclobutane ring alone, has not so far been observed. We now report that this dumb-bell-shaped molecule can be synthesized by a solid-state mechanochemical reaction of C_{60} with potassium cyanide. Our X-ray structural analysis shows that the C_4 ring connecting the cages is square rather than rectangular—the latter is predicted theoretically[8,9,13–15]. The dimer dissociates cleanly into two C_{60} molecules on heating or one-electron reduction, but in the gas phase during mass-spectrometric measurements it undergoes successive loss of C_2 units, shrinking to even-numbered fullerenes such as C_{118} and C_{116} in a sequence similar to that seen for other large fullerenes[19,20].

Recently, we developed a new method to derivatize C_{60} in the solid state by the use of a 'vibrating mill'[21]. The key feature of this method is a high-speed vibration technique, which can activate the reaction system by bringing the reagents into very close contact at the preparative scale and by providing extra mechanical energy, much more effectively than the ball-milling technique[22]. The reaction of C_{60} with KCN in the solid state has led to the first preparation of dumb-bell-shaped C_{120} (**1**) instead of formation of $C_{60}H(CN)$ (**2**)[23] after quenching with trifluoroacetic acid.

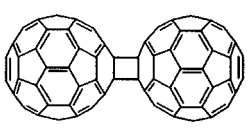

1

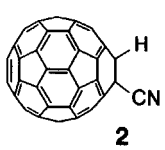

2

A mixture of C_{60} and 20 molar equivalents of KCN powder was vigorously vibrated for 30 min under nitrogen according to our previous procedure[21]. Analysis by high-performance liquid chromatography of the reaction mixture dissolved in *o*-dichlorobenzene (ODCB) on a Cosmosil Buckyprep column with toluene as the eluent showed only one major product besides unchanged C_{60}. Separation by flash chromatography on silica gel, eluted with hexane–toluene and then with toluene–ODCB, gave 70% of recovered C_{60} and 18% of C_{120} (**1**). Its structure was unequivocally determined as the [2 + 2] adduct of C_{60} based on the evidence shown below.

The product, isolated as a dark brown powder, has very low solubility in CS_2 and toluene, but is reasonably soluble (1–2 mg ml^{-1}) in ODCB. The ^{13}C NMR spectrum (Fig. 1) exhibited 15 signals (including one overlapped signal) in the sp^2 region and one signal at 76.22 p.p.m. in the sp^3 region, which are fully consistent with the assigned structure with D_{2h} symmetry. A comparison of the present data with the ^{13}C magic-angle spinning (MAS) NMR spectra of C_{60} polymers prepared under high pressure[24,25] has

established that the dumb-bell-shaped C_{120} is indeed the essential subunit of these polymers.

The Fourier-transform infrared spectrum of **1** showed more infrared-active peaks than C_{60} and resembled that of polymer prepared by photo-irradiation[7], thus giving a strong support for the presence of the [2 + 2] structure in the photoproduced polymer. Just like other 1,2-dihydro[60]fullerenes, the colour of **1** in toluene and in ODCB is brown. The ultraviolet–visible spectrum of **1** in toluene exhibited absorptions at 328, 434 and 698 nm, which are typical for 1,2-dihydrofullerene derivatives. The elemental analysis of **1** showed complete absence of any hydrogen or nitrogen.

Several mass-spectral techniques including fast atom bombardment (FAB), atmospheric pressure chemical ionization (APCI) and electrospray ionization (ESI) in both positive- and negative-ion modes did not show any molecular ion peak of **1** but a strong peak for C_{60}. Only a weak peak at mass/charge *m/z* 1,441 (M^+) together with a series of peaks corresponding to the loss of C_{2n} ($n = 1$–5) from C_{120} and a base peak at *m/z* 720 for C_{60} were observed in both Fourier-transform ion cyclotron resonance (FTICR) (Fig. 2) and matrix-assisted laser desorption-ionization (MALDI) time-of-flight mass spectra. This intriguing result indicates that C_{120} not only dissociates into C_{60} but also reduces its size by extruding C_2 units and rearranging into even-numbered fullerenes C_{118}, C_{116} and so on[19,20].

The structure of **1** was determined by X-ray crystallography for the single crystal grown in an ODCB solution. As shown in Fig. 3, dimer **1**

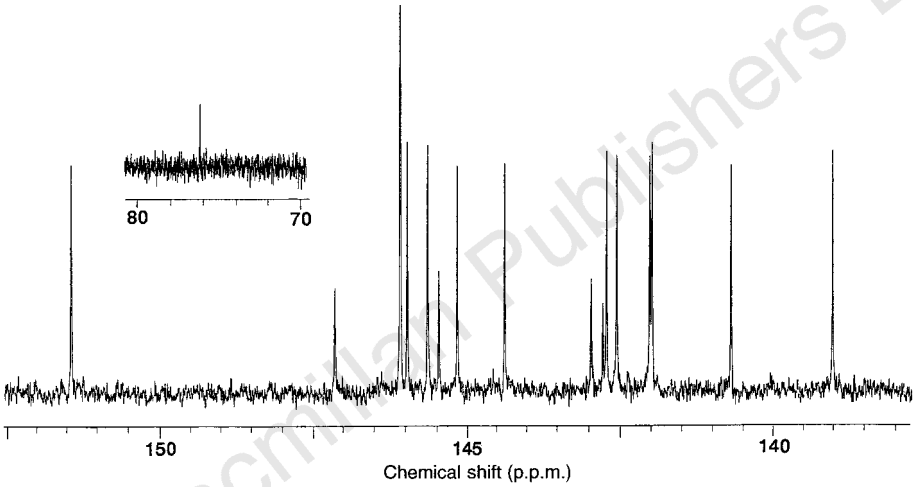

Figure 1 The ^{13}C NMR (150.8 MHz) spectrum of fullerene dimer **1** in ODCB-d_4: chemical shift δ (p.p.m.); 151.42 (8C), 147.14 (4C), 146.08 (8C × 2), 145.97 (8C), 145.65 (8C), 145.48 (4C), 145.18 (8C), 144.37 (8C), 142.97 (4C), 142.73 (8C), 142.56 (8C), 142.02 (8C), 141.99 (8C), 140.70 (8C), 139.02 (8C), 76.22 (4C). The signal at δ 142.79 p.p.m. is that of C_{60}.

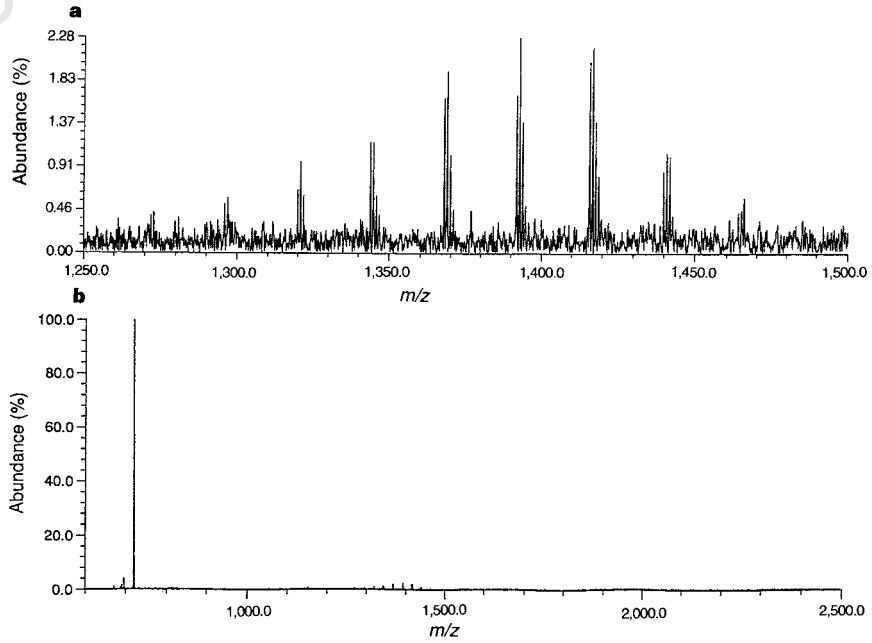

Figure 2 The positive-ion Fourier-transform ion cyclotron resonance (FTICR) mass spectra of fullerene dimer **1**. **a**, An expanded plot showing the molecular ion peak of C_{120} at *m/z* 1,441 (intensity 1.0%) (plus isotopic peaks) and a series of peaks for $C_{120} - C_{2n}$ ($n = 1$–5), that is, *m/z* 1,417 (C_{118}, 2.2%), 1,393 (C_{116}, 2.3%), 1,369 (C_{114}, 1.9%), 1,345 (C_{112}, 1.2%) and 1,321 (C_{110}, 1.0%). The spectrum also exhibits a very weak peak at *m/z* 1,465, which indicates the formation of a small amount of C_{122} by the process of $C_{120} + C_2$. **b**, A full-range spectrum showing a base peak for C_{60} at *m/z* 720 (intensity 100%) and a cluster of peaks around *m/z* 1,440.

is composed of two C_{60} cages sharing a cyclobutane ring. Previous theoretical studies predicted the intra-cage bond (C1–C2 in Fig. 3) to be rather long (1.59–1.62 Å)[8,913–15] compared with the inter-cage bond (C1–C1* in Fig. 3). Present results show that there is no great difference in the length of these bonds. The former bond length is 1.581(7) Å, which is rather short compared to reported values for the corresponding bond in substituted 1,2-dihydrofullerenes[26]. The relative elongation of the inter-cage bond (1.575(7) Å) compared with the ordinary $C(sp^3)$–$C(sp^3)$ single bond is well reflected in its ready thermal cleavage, as will be discussed below.

Differential scanning calorimetry was used to follow the thermal behaviour of **1** in the range 80–220 °C at a rate of 1 °C min^{-1}. An endothermic peak from 150 to 175 °C and centred at 162 °C was observed in the heating process, whereas no such peak was observed in the cooling scan. Moreover, C_{120} was found to dissociate quantitatively into C_{60} by heating its ODCB solution at 175 °C for 15 min. This decomposition temperature is near to those reported for polymers prepared by photo-irradiation[27] and under high pressure[28,29].

Cyclic voltammetry of **1** (0.25 mM in ODCB/0.05 M Bu_4NBF_4; Pt disk and Pt wire as working and counter electrodes, respectively; scan rate, 20 mV s^{-1}) exhibited three reversible reductions at $E_{1/2}$ −1.14, −1.53 and −1.99 V versus ferrocene/ferrocenium, which are almost the same as those of C_{60} (−1.12, −1.52 and −1.99 V) observed under the same conditions. The only noticeable difference in the electrochemical behaviour between **1** and C_{60} is the presence of a small shoulder at the first reduction peak of **1** in both cyclic voltammetry and differential pulse voltammetry. Taken together, these results indicate that dimer **1** readily dissociates into the C_{60} anion radical and C_{60} immediately after C_{120} acquires one negative charge.

The very close reduction potentials of C_{120} and C_{60} suggests that C_{120} should have equal chemical reactivity to C_{60}. In fact, the versatile Bingel reaction[30] was found to be able to functionalize **1**. Reaction of dimer **1** in ODCB solution with one equivalent each of diethyl bromomalonate and 1,8-diazabicyclo[5.4.0]undec-7-ene for 30 min at room temperature afforded monoadduct of **1** in 44% yield along with 24% of unchanged **1** after separation on JAIGEL − 1H + 2H preparative gel permeation chromatography (GPC) columns eluted with toluene. The adduct was a mixture of at least three positional isomers as judged from HPLC and ^{1}H NMR data.

The dimerization of C_{60} did not take place without KCN in the solid state. Furthermore, no cyanated product **2**[23] was isolated in the solid-state reaction of C_{60} with KCN. The highly selective synthesis of C_{120} observed here is ascribed to a reaction pathway totally different from that in the liquid phase[23], and to the unique property of cyanide ion behaving both as a nucleophile and as a good leaving group. The solid-state reactions of C_{60} with other nucleophiles did not afford C_{120} (ref. 21). We suppose that the present dimerization

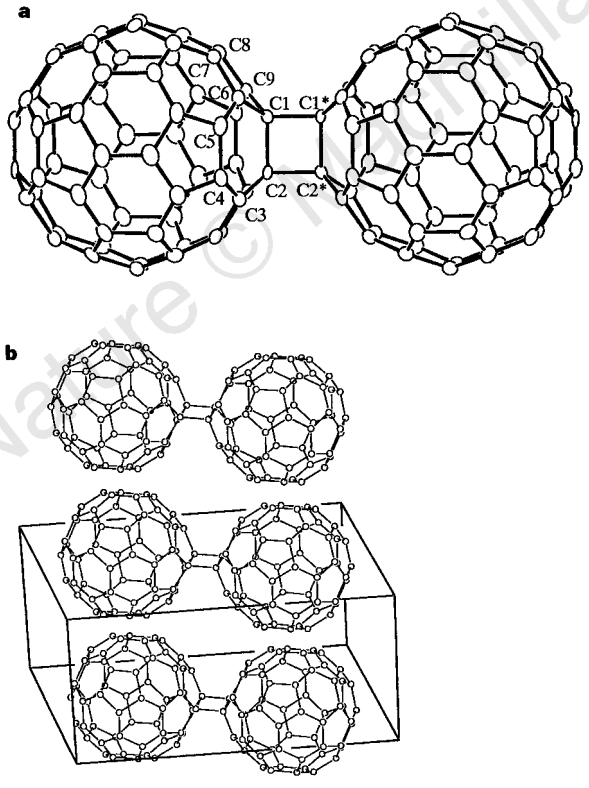

Figure 3 a, Structure of fullerene dimer **1**, as determined by X-ray crystallography. Selected bond lengths (Å) and angles (degrees) are: C1–C1*, 1.575(7); C1–C2, 1.581(7); C2–C3, 1.530(8); C3–C4, 1.374(7); C4–C5, 1.468(8); C5–C6, 1.358(9); C6–C1, 1.528(7); C6–C7, 1.445(8); C7–C8, 1.457(9): C2–C1–C6, 115.4(5); C2–C1–C9, 115.2(4); C6–C1–C9, 100.7(4); C2–C1–C1*, 90.3(4); C1–C2–C2*, 89.7(4). **b**, A crystal packing diagram. The R and R_w values were 0.067 and 0.096, respectively. The solvent molecules were contained in a 4 : 1 ratio in the crystal of **1**, but are omitted from these figures for clarity. Further material characterizing **1**, including X-ray structure details, are available as Supplementary Information.

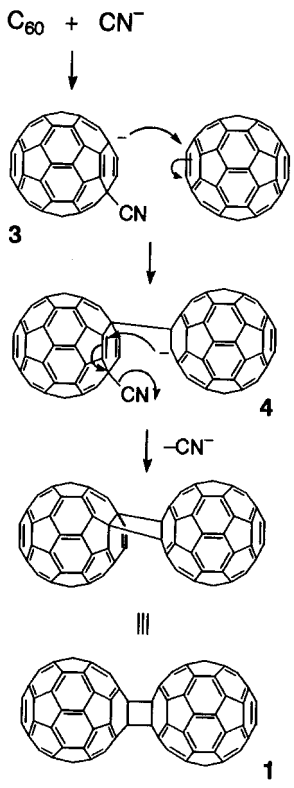

Figure 4 Proposed reaction mechanism for the formation of dimer **1**.

occurs in a similar fashion to the so-called benzoin condensation[31]. As shown in Fig. 4, cyanide ion first adds to C_{60} to form $C_{60}(CN)^-$ (**3**), which can react with the closely located molecule of C_{60} in the 1,4-addition mode to minimize steric congestion and gives anion **4**. Then an intramolecular S_N2' reaction of **4** furnishes the [2 + 2] dimer **1**. A further reaction of dimer **1** with cyanide ion could occur, but this would make **1** acquire a negative charge together with a cyano group, and would cause the rupture of its [2 + 2] bonds as inferred from the above-mentioned electrochemical behaviour of **1**. Thus the overall reaction results in the highly selective formation of dimer C_{120} instead of oligomers and polymers.

In single crystals of **1** obtained in the present study, the C_{120} molecules are arrayed in highly ordered layers, different from the face-centred cubic arrangement of C_{60}. Photo-irradiation of this crystalline material should lead to the formation of a C_{60} polymer, which might have a more well-defined structure than previously reported ones[7,32]. The present result indicates that a thermally forbidden [2 + 2] process of a highly electron-deficient and strained double bond such as that in fullerenes can take place under solid-state reaction conditions catalysed by cyanide ion. Application of the present method to C_{70} is expected to lead to another new carbon allotrope, C_{140}. □

Received 28 January; accepted 22 April 1997.

1. *Acc. Chem. Res.* (spec. iss. on buckminsterfullerenes) **25,** 97–176 (1992).
2. Billups, W. E. & Ciufolini, M. A. (eds) *Buckminsterfullerenes* (VCH, New York, Weinheim, 1993).
3. Kroto, H. W., Fischer, J. E. & Cox, D. E. (eds) *The Fullerenes* (Pergamon, Oxford, 1993).
4. Prassides, K. (ed.) *Physics and Chemistry of the Fullerenes* (NATO ASI Ser., Kluwer Academic, Dordrecht, 1994).
5. Kuzmany, S., Fink, J., Mehring, M. & Roth, S. (eds) *Progress in Fullerene Research* (World Scientific, Singapore, 1994).
6. Taylor, R. (ed.) *The Chemistry of Fullerenes* (World Scientific, Singapore, 1995).
7. Rao, A. M. *et al.* Photoinduced polymerization of solid C_{60} films. *Science* **259,** 955–957 (1993).
8. Strout, D. L. *et al.* A theoretical study of buckminsterfullerene reaction products C_{60} + C_{60}. *Chem. Phys. Lett.* **214,** 576–582 (1993).
9. Matsuzawa, N., Ata, M., Dixon, D. A. & Fitzgerald, G. Dimerization of C_{60}: the formation of dumbbell-shaped C_{120}. *J. Phy. Chem.* **98,** 2555–2563 (1994).
10. Menon, M., Subbaswamy, K. R. & Sawtarie, M. Structure and properties of C_{60} dimers by generalized tight-binding molecular dynamics. *Phys. Rev. B* **49,** 13966–13969 (1994).
11. Adams, G. B., Page, J. B., Sankey, O. F. & O'Keeffe, M. Polymerized C_{60} studied by first-principles molecular dynamics. *Phys. Rev. B* **50,** 17471–17479 (1994).
12. Porezag, D., Pederson, M. R., Frauenheim, T. & Köhler, T. K. Structure, stability, and vibrational properties of polymerized C_{60}. *Phys. Rev. B* **52,** 14963–14970 (1995).
13. Kürti, J. & Németh, K. Structure and energetics of neutral and negatively charged C_{60} dimers. *Chem. Phys. Lett.* **256,** 119–125 (1996).
14. Scuseria, G. E. What is the lowest-energy isomer of the C_{60} dimer? *Chem. Phys. Lett.* **257,** 583–586 (1996).
15. Osawa, S., Sakai, M. & Osawa, E. Nature of cyclobutane bonds in the neutral [2 + 2] dimer of C_{60}. *J. Phys. Chem. A* **101,** 1378–1383 (1997).
16. Lebedkin, S., Ballenweg, S., Gross, J., Taylor, R. & Krätschmer, W. Synthesis of $C_{120}O$: a new dimeric [60]fullerene derivative. *Tetrahedr. Lett.* **36,** 4971–4974 (1995).
17. Smith, A. B., Tokuyama, H., Strongin, R. M., Furst, G. T. & Romanow, W. J. Synthesis of oxo- and methylene-bridged C_{60} dimers, the first well-characterized species containing fullerene-fullerene bonds. *J. Am. Chem. Soc.* **117,** 9359–9360 (1995).
18. Gromov, A. *et al.* $C_{120}O_2$: The first [60]fullerene dimer with cages bis-linked by furanoid bridges. *J. Chem. Soc. Chem. Commun.* 209–210 (1997).
19. Yeretzian, C., Hansen, K., Diederich, F. & Whetten, R. L. Coalescence reactions of fullerenes. *Nature* **359,** 44–47 (1992).
20. Ata, M., Takahashi, N. & Nojima, K. Mass peak assignment for C_{60} polymer generated in an Ar plasma. *J. Phys. Chem.* **98,** 9960–9965 (1994).
21. Wang, G.-W., Murata, Y., Komatsu, K. & Wan, T. S. M. The solid-phase reaction of [60]fullerene: novel addition of organozinc reagents. *J. Chem. Soc. Chem. Commun.* 2059–2060 (1996).
22. Braun, T. *et al.* Mechanochemistry: a novel approach to the synthesis of fullerene compounds. Water soluble buckminsterfullerene-γ-cyclodextrin inclusion complexes via a solid-solid reaction. *Solid State Ionics* **74,** 47–51 (1994).
23. Keshavarz-K., M., Knight, B., Srdanov, G. & Wudl, F. Cyanodihydrofullerenes and dicyanodihydrofullerene: the first polar solid based on C_{60}. *J. Am. Chem. Soc.* **117,** 11371–11372 (1995).
24. Persson, P.-A. *et al.* NMR and Raman characterization of pressure polymerized C_{60}. *Chem. Phys. Lett.* **258,** 540–546 (1996).
25. Goze, C. *et al.* High-resolution ^{13}C NMR studies of high-pressure-polymerized C_{60}: evidence for the [2 + 2] cycloaddition structure in the rhombohedral two-dimensional C_{60} polymer. *Phys. Rev. B* **54,** R3676–R3678 (1996).
26. Ishida, T., Shinozuka, K., Nogami, T., Sasaki, S. & Iyoda, M. First X-ray structural determination of fullerene [2 + 2] cycloadduct. *Chem. Lett.* 317–318 (1995).
27. Wang, Y., Holden, J. M., Bi, X.-X. & Eklund, P. C. Thermal decomposition of polymeric C_{60}. *Chem. Phys. Lett.* **217,** 413–417 (1994).
28. Yamawaki, H. *et al.* Infrared study of vibrational property and polymerization of C_{60} and C_{70} under pressure. *J. Phys. Chem.* **97,** 11161–11163 (1993).
29. Núñez-Regueiro, M., Marques, L., Hodeau, J.-L., Béthoux, O. & Perroux, M. Polymerized fullerene structures. *Phys. Rev. Lett.* **74,** 278–281 (1995).
30. Bingel, C. Cyclopropanierung von Fullerenen. *Chem. Ber.* **126,** 1957–1959 (1993).
31. March, J. *Advanced Organic Chemistry* 4th edn 969–970 (Wiley, New York, 1992).
32. Sun, Y.-P., Ma, B., Bunker, C. E. & Liu, B. All-carbon polymers (polyfullerenes) from photochemical reactions of fullerene clusters in room-temperature solvent mixtures. *J. Am. Chem. Soc.* **117,** 12705–12711 (1995).

Supplementary Information is available on *Nature*'s World-Wide Web site (http://www.nature.com) or as paper copy from Mary Sheehan at the London editorial office of *Nature*.

Acknowledgements. We thank K. Yamamoto of Power Reactor and Nuclear Fuel Development Corporation for measuring FT ICR MS spectra; S. Sugiura for the use of a ^{13}C NMR spectrometer; Y. Tsujii for assistance with DSC measurements; and S. F. Nelsen (Univ. Wisconsin) and K. Tamao for discussions and encouragement. This work was supported by the Japan Society for the Promotion of Science and the Ministry of Education, Science and Culture, Japan.

Correspondence and requests for materials should be addressed to K.K. (e-mail: komatsu@scl.kyoto-u.ac.jp).

The Lu–Hf dating of garnets and the ages of the Alpine high-pressure metamorphism

S. Duchêne, J. Blichert-Toft, B. Luais, P. Télouk, J.-M. Lardeaux & F. Albarède

Ecole Normale Supérieure de Lyon and Université Claude-Barnard, UMR-CNRS 5570, 69364 Lyon cedex 7, France

It remains controversial whether burial and exhumation in mountain belts represent episodic or continuous processes[1–20]. Regional patterns of crystallization and closure ages of high-pressure rocks may help to discriminate one mode from the other but, unfortunately, metamorphic geochronology suffers from several limitations. Consequently, no consensus exists on the timing of high-pressure metamorphic events, even for the Alps—which have been the subject of two centuries of field work. Here we report lutetium–hafnium (Lu–Hf) mineral ages on eclogites from the Alps as obtained by plasma-source mass spectrometry. We find that the Lu/Hf ratio of garnet is particularly high, which helps to provide precise ages. Eclogites from three adjacent units of the western Alps give (from bottom to top) diachronous Lu–Hf garnet ages of 32.8 ± 1.2, 49.1 ± 1.2 and 69.2 ± 2.7 Myr. These results indicate that the Alpine high-pressure metamorphism did not occur as a single episode some 80–120 Myr ago[6,7,10,18], but rather that burial and exhumation represent continuous and relatively recent processes.

With the discovery of the coesite-bearing quartzites of Dora Maira in the western Italian Alps[1], the exhumation history of rocks that had been buried to ~100 km depth during the formation of the Alps provided fresh insight into alpine tectonic processes. Published data, however, emphasize both the extent of inconsistency of the chronological data on high-pressure metamorphism and its far-reaching geodynamic implications[2–5]. The Eoalpine age (100–120 Myr) inferred from a discordant array of zircons[6] and from ^{39}Ar–^{40}Ar dating in phengites[7,8] seems to support a widely accepted view that the exhumation of eclogites is coeval with the continuing subduction of the oceanic Tethyan lithosphere under the African plate[9]. Eclogite burial and exhumation also appear to be Eoalpine in age in the Sesia-Lanzo unit with Rb–Sr, K–Ar and U–Pb ages in the range 60–114 Myr (refs 10–12). In contrast, the Late Eocene–Early Oligocene age found for Dora Maira[13,14]—as a lower concordia intercept defined by zircons and as a U–Pb isochron on ellenbergerite, which was later confirmed by U–Pb ion-probe data on zircons[15]—rather suggests that burial and exhumation are far more recent and coeval with the collision between the Apulian and European plates. Sm–Nd and U–Pb Eocene ages are also known from other eclogite localities in the western and central Alps[16–18]. As these eclogites seem to have been overprinted in the greenschist facies during the Oligocene (25–35 Myr ago) at the latest[7,19], the value of the exhumation rate may vary from a fraction of a millimetre to several centimetres per year depending on which age is accepted for the high-pressure metamorphism.

Other than K–Ar, of which the significance is obscured by the